CHEMISTRY
A European Journal

A Journal of
ChemPubSoc Europe

Accepted Article

Title: Bistable Solid-State Fluorescence Switching in Photoluminescent Infinitely Coordinated Polymer

Authors: Jincheol Kim, Youngmin You, Seong-Jun Yoon, Jong H. Kim, Boseok Kang, Sang Kyu Park, Dong Ryeol Whang, Jangwon Seo, Kilwon Cho, and Soo Young Park

To be cited as: *Chem. Eur. J.* 10.1002/chem.201701656

Link to VoR: http://dx.doi.org/10.1002/chem.201701656

Supported by
ACES

WILEY-VCH

10.1002/chem.201701656

WILEY-VCH

Bistable Solid-State Fluorescence Switching in Photoluminescent Infinitely Coordinated Polymer

Jincheol Kim,[a] Youngmin You,[b] Seong-Jun Yoon,[a] Jong H. Kim,[c] Boseok Kang,[d] Sang Kyu Park,[a] Dong Ryeol Whang,[a] Jangwon Seo,[a] Kilwon Cho,[d] and Soo Young Park*[a]

Abstract: Photo-functional infinitely coordinated polymers (ICPs) consisting of the photochromic dithienylethene (DTE) and the luminescent bridging unit to give enhanced fluorescence in the solid state were synthesized. We could fabricate well-ordered micropatterns of these ICPs by a soft-lithographic method, which repeatedly showed high contrast on-off fluorescence switching.

Metal–ligand coordination provides a unique strategy to construct functional polymers, as the coordination geometry directs facile formation of well-defined, multidimensional networks.[1] Metal–organic frameworks (MOFs) are the most prominent material class among the coordination polymers, because their reticular inner structures render interesting functions such as storage or separation of guest molecules.[2] However, MOFs do not carry the full merit of the metal–ligand coordination because the brittle structures are seldom compatible with solution processes. In addition, the prevalent solvothermal synthetic method to attain MOFs manifests a severe limitation, i.e., difficulties for finding ligand structures that can be incorporated into the polymeric structure. On the other hand, ICPs with reversible coordination bonds are considered as promising alternatives to MOFs, in the context of versatility and processibility.[3] ICPs can readily be prepared under mild condition, and their synthetic procedures feature excellent flexibility in the selection of a wide range of metal ions and bridging ligands. The latter feature is particularly beneficial because it allows broad control over physical and chemical properties. Indeed, several classes of ICPs have been prepared and demonstrated for potential use in catalysis,[4] drug delivery,[5] and sensing.[6]

[a] J. Kim, Dr. S. -J. Yoon, Dr. J. H. Kim, Dr. S. K. Park, Dr. D. R. Whang, Dr. J. Seo, Prof. S. Y. Park*
Center for Supramolecular Optoelectronic Materials and Department of Materials Science and Engineering
Seoul National University
Daehak-dong, Gwanak-gu, Seoul, Korea
E-mail: parksy@snu.ac.kr
[b] Prof. Y. You
Division of Chemical Engineering and Materials Science
Ewha Womans University
Seoul 03760, Korea
[c] Prof. Jong H. Kim
Department of Molecular Science and Technology,
Department of Applied Chemistry and Biological Engineering,
Ajou University
Suwon 443-749, Korea
[d] B. Kang, Prof. K. Cho
Department of Chemical Engineering
Pohang University of Science and Technology
Pohang 790-784, Korea

Supporting information for this article is given via a link at the end of the document.

Incorporation of photoluminescent ligands into the coordination networks of ICPs provides a useful way to the preparation of solid-state luminescent materials. The ability to locate photoluminescent ligands within the multidimensional space is advantageous over conventional organic polymers that suffer from detrimental photoluminescence quenching due to nonspecific inter-chain interactions in the solid state. Despite this advantage, demonstration of fluorescent ICPs has seldom been reported.[7] However, we could recently report fluorescent micropatterns of ICPs using a soft-lithographic micromolding in capillaries (MIMIC) technic, which is a simple yet very effective method for nano-/micro-structures fabrications.[8] The ICP is comprised of diamagnetic zinc ions and bridge ligands having 4-pyridyl moieties at both termini. Fluorescence intensity of the ICP was much stronger than that of the ligand solution, which was attributed to the suppressed vibronic relaxation due to coordination-induced restriction of intramolecular motions.

Having previously demonstrated the promising utility of fluorescent ICPs, we sought to extend their capability by incorporating the second photofunctional ligands into the ICP backbones in this work. This approach is reminiscent of statistical copolymers. We chose photochromic DTE compounds as the second ligands to demonstrate an all-optical solid-state fluorescence memory, because the photochromism of the DTE compounds features many advantages, including high thermal stability, good fatigue resistance, and excellent reversibility.[9] The actual photochromism involves optical interconversion between the open and closed forms of DTE, where the latter exhibits strong absorption in the visible region ($\varepsilon > 10^4$ M^{-1} cm^{-1}). Thus, fluorescence quenching by interligand energy transfer (most likely by a Förster resonance energy-transfer mechanism as reported before) [9b-d, 10] from the fluorescent ligand to the closed form of the DTE ligand is anticipated. Photochromic cycloreversion to the open form of DTE restores the strong fluorescence, completing the fluorescence memory cycle. It should be noted that the individual operation of writing, reading, and erasing can be done in an all-optical manner with minimal crosstalks. This can be led from the negligible absorption cross-section of both closed and open forms of DTE at the photoluminescence excitation wavelength of the aggregation-induced enhanced emission (AIEE) type bridge ligand (430 nm). Furthermore, the solid-state memory retains the full advantage of ICPs, as it can be reconfigured using solution processes to prepare various bulk structures, such as films and micropatterns (see Scheme 1). To the best of our knowledge, this is the first report on bistable solid-state fluorescence memory based on ICPs synthesized by non-solvothermal synthetic method. Herein, we report the design and synthesis of novel ICPs containing zinc ions, fluorescent (Z)-2,3-bis(4-(4-pyridinyl)phenyl)acrylonitrile (**L1**)

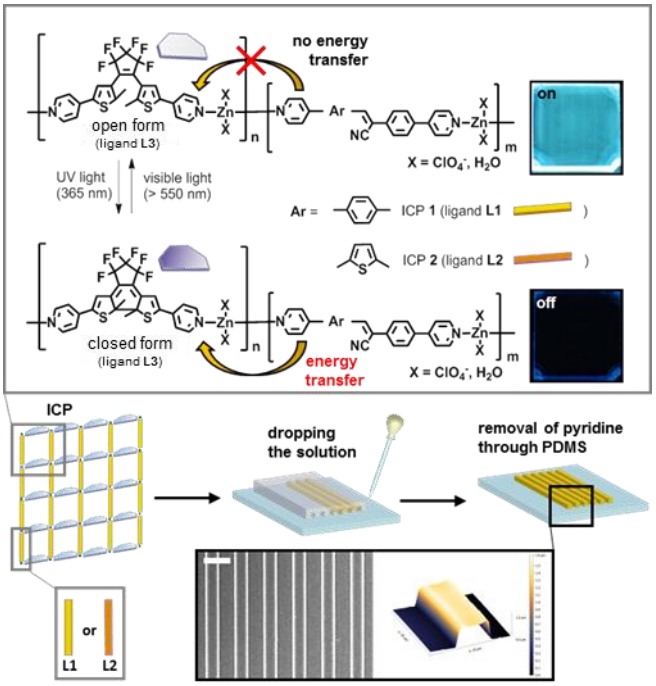

Scheme 1. Illustration of energy transfer concept of ICP1 and ICP2 (not the proposed structure of ICP), and the schematic representation of the fabrication of micropatterns of ICP by the MIMIC method. Inset images on the bottom show the FE-SEM and AFM images of the micro-line/space patterns of ICP1. (scale bar = 20 μm)

(Z)-2-(4-(4-pyridineyl)phenyl)-3-(5-(pyridine-4-yl)thiophen-2-yl) acrylonitrile (**L2**) ligands, and a photochromic 1,2-bis(2-methyl-5-(4-pyridyl)-3-thienyl)perfluorocyclopentene (**L3**) ligand (Supporting Information (SI), Scheme S1-S3).

The AIEE-active (**L1**) and photochromic DTE (**L3**) ligands were synthesized according to the method described previously in the literature.[11] To maximize the interligand energy transfer efficiency, we also synthesized AIEE-active **L2** ligand by substituting the phenyl ring in L1 with thiophene, which is responsible for a red-shifted fluorescence emission of **ICP2**. In these ligand structures, Lewis-basic moieties were kept identical to be 4-pyridine to guarantee even incorporation of the ligands into the polymer networks. All compounds were fully characterized by ^{1}H and ^{13}C NMR spectroscopy, MS spectrometry, and elemental analysis (SI).

ICP1 was prepared by slowly adding 1 mL of 200 μM $Zn(ClO_4)_2$ (MeOH) into a stirred 10 mL CH_2Cl_2 solution containing 100 μM **L1** and 100 μM **L3**. The mixture was then stirred for additional 12 h. The supernatant was removed by decantation, and the powders were collected by filtration and thoroughly washed with dichloromethane and water to remove residual ligands and zinc ions. **ICP2** was obtained through the identical procedure, employing 100 μM **L2** instead of **L1**. FT–IR data for ICP pellets display absorption bands at 1614 cm^{-1} due to zinc-coordinated pyridine, which is distinct from that (1595 cm^{-1}) of free pyridine (SI, Figure S1).[12] Incorporation of the zinc ions in the ICP backbones was verified by XPS analysesas reported previously.[8] The XPS data display sharp peaks due to Zn(2*p*), S(2*p*), F(1*s*), and N(1*s*), where the relative abundance of these species are 1.03%, 1.92%, 6.3%, and 5.35%, respectively, for **ICP1**. To quantify ligands, each component is calculated by counting elements such as N(1s) or F(1s) as shown in supporting information. It should be noted that corresponding co-monomer ratio for (**L1** + **L3**) / Zn is determined to be 2.07 which implies **ICP1** possess 2D or 3D alternating (zinc-ligand) backbone structures similar to our previous ICP comprising solely **L1** ligand. The authors argue that formation of the multidimensional structure is allowed by the weakly coordinating perchlorate ion of zinc.[8] **ICP2** exhibits a co-monomer ratio for (**L2** + **L3**) / Zn = 0.94 and these values suggest that the ICPs possibly contained 0D or 1D wire coordination structures (SI, Table S1). Since the thiophene moiety does not compete with 4-pyridine moiety for the coordination polymerization, it is most likely that the lower dimensional characteristic of **ICP2** is caused by non-linear ligand geometry caused by substitution of thiophene instead of pheynyl moiety which could hinder the formation of higher multidimensional network. It is also noteworthy to mention that the co-monomer ratios in these pristine powders of **ICP1** and **ICP2** are lower than those in the regenerated MIMIC patterns (*vide infra*) attributed to the different crystallization condition as mentioned later.

Treatments of the ICP powders with an excess amount of pyridine led to the complete de-coordination of the bridging ligands. The coordination bonds would then be recovered by selective removal of pyridine, due to reversible coordination. We combined this depolymerization-repolymerization principle and the MIMIC technic. Since ordering in supramolecular structures and bulk morphology is crucial for attaining enhanced optoelectronic properties, such as high carrier mobility and fluorescence quantum yields of solid-state devices, the combined approach is expected to provide a unique advantage for fabrication of the microscale patterns with three dimensional coordination structures.[8] To fabricate micropatterns, pyridine solutions (1000 mg) containing 20 mg of **ICP1** or **ICP2** were prepared. The solutions were injected into the rectangular capillary channels which were formed by conformal contact between a negatively pre-patterned poly(dimethylsiloxane) (PDMS, Sylgard 184, Dow Corning) mold and a glass substrate. At the inner walls of the capillaries, pyridine solvent was selectively absorbed by the PDMS mold, regenerating and furnishing ICPs inside the mold channels.[8] Peeling off the mold from the glass substrate after full pyridine absorption into PDMS mold produced micro-patterned coordination polymer wires arrays (Scheme 1).

Field-emission scanning electron microscope (FE-SEM) and atomic force microscope (AFM) images reveal the flat surface of the ICP micropatterns with negligible shrinkage (SI, Figure S2). The patterned ICPs were insoluble in dichloromethane and chloroform, whereas ligand micropatterns prepared through the identical MIMIC technique (i.e., no zinc ions) were dissolved out by those solvents (SI, Figure S3). Unidirectional property of a patterned wire is further evaluated from the strong birefringence observed using an optical microscope under a cross-polarized condition (SI, Figure S3). Assays based on XPS data revealed retention of multidimensional structures (i.e., 2D net; SI, Table S1). Interestingly, the ligand/Zn ratios (2.65 for **ICP1**) for the MIMIC micropatterns were significantly larger than that of the as-

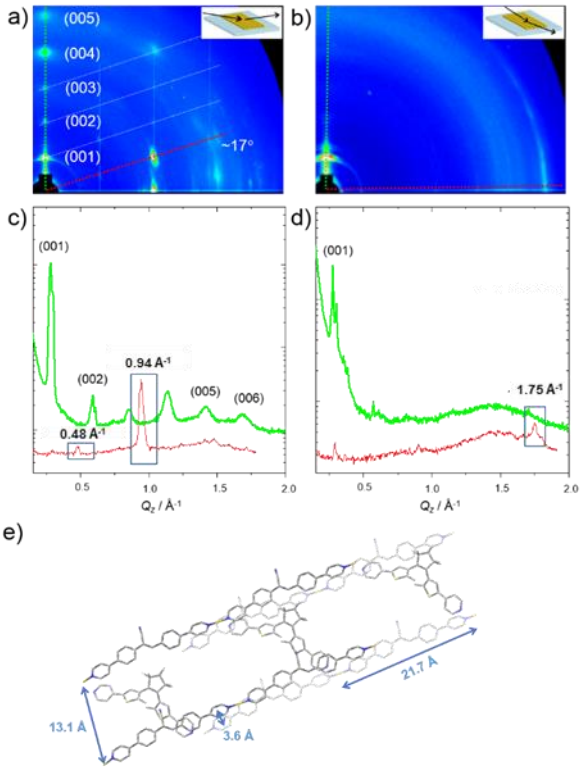

Figure 1. 2D GIXD of coordination polymer patterns of **ICP1** in a) the vertical direction and b) horizontal direction. c) 1D out-of-plane (green line) and 17° direction (red line) X-ray profile extracted from lines of (a). d) 1D out-of-plane (green line) and in-plane (red line) X-ray profile extracted from (b). e) Representation of a possible coordination geometry which can be predicted from the 2D GIXD results. Nitrogen and zinc are represented by blue and orange atoms. Counteranions and hydrogen are omitted for clarity.

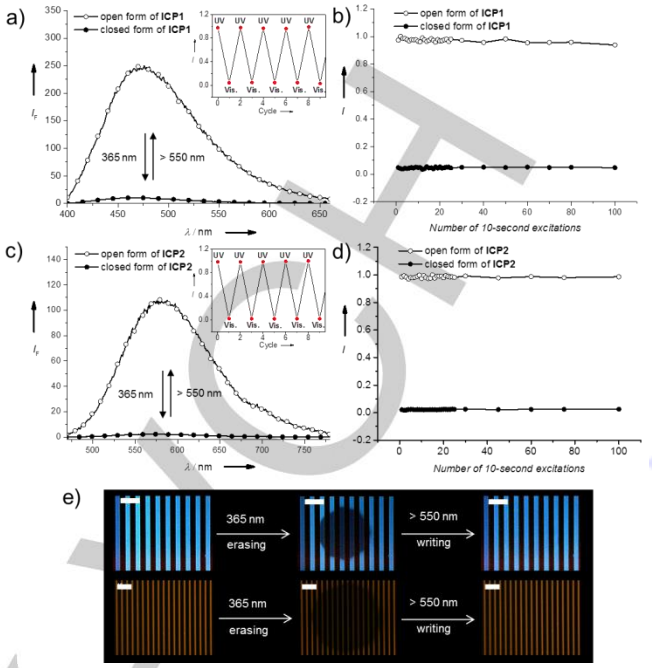

Figure 2. PL spectra of a) **ICP1** and c) **ICP2** in the open (open circles) and closed (filled circles) DTE states, and photoluminescence intensities of b) **ICP1** and d) **ICP2** upon repeative exposure of the photoexcitation beam (λ_{ex} = 430 nm). Inset graphs show the photochromic modulation of photoluminescence of **ICP1** and **ICP2** films. e) photo-switchable fluorescence images of the micropatterns of **ICP1** (blue) and **ICP2** (orange) (Scale bar = 40 μm).

prepared powders (2.01) which suggests that the micro-patterned ICPs possess higher dimensional coordination structures. This presumably originates from controlled repolymerization inside the capillary channels, providing longer crystallization time in a confined space to give highly-oriented coordination polymer.

We measured 2D grazing incidence X-ray diffraction (2D GIXD) of the patterned **ICP1** to obtain the detailed structural information. Different from the previously reported jungle gym-like cubic structure composed solely of a fluorophore (L1) and zinc,[8] the patterned **ICP1** showed crystalline anisotropy depending on measuring directions. When the X-ray beam is injected for a perpendicular direction to the line patterns (Figure 1a), strong (00k) diffraction peaks appear along the out-of-plane direction up to the 5th order, which corresponds to the d-spacing value of 21.7 Å. This value matches well with the length of ligand **L1** (SI, Figure S4). Furthermore, the 2D GIXD pattern at the perpendicular direction shows the unique oblique parallelogram structure with an angle of ~17° with respect to the substrate. The 1D diffraction intensity profile extracted at ~17° direction displays two peaks at q = 0.48 and 0.94 Å^{-1}, in which the length value of 13.1 Å calculated from these peaks is shorter than that of the used ligands. The 2D GIXD pattern of the patterned **ICP1** measured at the horizontal direction showed apparently different crystalline feature (Figure 1b and 1d). The notable difference appears at 1.75 Å^{-1} at the in-plane direction (a d-spacing of 3.8 Å), which can be attributed to **π-π** stacking of the conjugated ligands. Considering all the information described above and the supporting information as well as the calculation results using the principles of quantum chemistry (SI, Figure S5), we could suggest a most probable structure of patterned **ICP 1**. As shown in Figure 1e, photochromic ligand **L3** is placed between the parallelogram structure of ligand **L1**. In case of **ICP2**, we were unable to get the strong diffraction peak from GIXD. This should originate from the lower multidimensional feature compared to **ICP1** which is consistent with the lower co-monomer ratio from XPS data as we mentioned previously. Because **ICP2** has the virtually similar length of ligand molecule, insolubility of pattern, and birefringence in the pattern of **ICP1**, we may suppose the lower multidimensional characteristic is caused by non-linear geometry of ligand **L2**.

Before the investigation of the fluorescence switching properties, we performed the structure analyses on the ICPs in the regenerated film state. We prepared 2 wt% **ICP1** and **ICP2** solutions in pyridine and fabricated photochromic fluorescent ICP films by spin-coating (700 rpm for 60 s). FT–IR spectra for the films display strong absorption peaks at 1616 cm^{-1}, indicating retention of Zn–ligand bonds (SI, Figure S7).[12] XPS analyses for the Zn(2*p*), S(2*p*), F(1*s*) and N(1*s*) elements in **ICP1** and **ICP2** reveal comonomer ratios of (AIEE ligands + DTE ligand) / zinc ions to be 2.40 and 1.15, respectively. These values correspond to multidimensional structures that involve 3D

or 2D nets for **ICP1** and 1D or 2D nets for **ICP2** (SI, Table S2) which are similar to but somewhat different from those of the micropatterns. It is noted that the co-monomer ratios in these thick films are slightly lower than those in the micro-patterned structures, probably due to the faster repolymerization process compared to that in the confined environment (inside of the PDMS mold channels).

The open and closed forms of the DTE photochrome for fluorescence switching in ICP patterns were generated by irradiating visible (λ > 550 nm) and UV (λ = 365 nm) light, respectively. The cyclization yields for the photo-stationary state (PSS) under irradiation with 365 nm light was estimated to be 38% and 34% for **ICP1** and **ICP2,** respectively, as determined by ^{1}H NMR spectroscopy (SI, Figure S7). The photochromism for the open and closed states of ICPs were completely reversible with distinct quantum yields (**ICP1**: $\Phi_{pc}^{o\rightarrow c}$ = 0.027, $\Phi_{pc}^{c\rightarrow o}$ = 0.0013; **ICP2**: $\Phi_{pc}^{o\rightarrow c}$ = 0.011, $\Phi_{pc}^{c\rightarrow o}$ = 0.001), similar to those of reported DTE compounds.[9a, 13] Strong fluorescence emission was observed with the open forms of the ICPs (**ICP1**: λ_{em} = 470 nm, PLQY = 0.18; **ICP2**: λ_{em} = 577 nm, PLQY = 0.19) when photoexcitation at 365 nm was provided, whereas fluorescence was barely detected with closed form of the ICPs (Figure 2). The large fluorescence quenching in the closed forms is likely attributed to the fluorescence resonance energy transfer (FRET) from the AIEE ligand to the closed form of the photochromic ligand having significantly low energy absorption band (*vide infra*; ligand centered absorption of **L3**; λ_{abs} = 613 nm; SI, Figure S8). Corresponding fluorescence on/off ratios for **ICP1** and **ICP2** are 24 and 47, respectively. Most intriguingly, as shown in the graphs of Figure 2b and 2d, the fluorescence intensities of these two isomeric states could remain completely unaltered, if the excitation is made by the non-destructive read-out beam (λ_{ex} = 430 nm). These results demonstrate that the ICP micropatterns are promising for optical memory materials (Figure 2e).

To gain information about the energy transfer processes, steady-state and transient PL were studied. UV–vis absorption and fluorescence spectra of 20 μM ligand solutions were recorded, which revealed fairly good spectral overlaps between the absorption spectrum of the closed form of **L3** and the fluorescence spectra of **L1** and **L2** ligands (SI, Figure S9)**.** Spectral overlap integrals for the pair of **L2** and **L3** is 4.73 $\times$ 10^{14} M^{-1} cm^{-1} nm^4, while that of **L1** and **L3** is relatively small (1.4 $\times$ 10^{14} M^{-1} cm^{-1} nm^4). This ordering is consistent with the fluorescence on/off ratios of the ICP micropatterns. We also monitored the occurrence of energy transfer by recording fluorescence decay traces of the ICP films in their open and closed forms (SI, Figure S10). The decay traces followed a multi-exponential kinetics due to heterogeneity of the ligands in the ICP networks. We found that the average fluorescence lifetimes (τ) of **ICP1** decreased from 0.83 ns to 0.26 ns upon photocyclization, while that of **ICP2** displayed a larger decrease (1.37 ns to 0.33 ns). The rate constants for energy transfer were calculated using the τ values ($k_{ET} = 1/\tau_{closed} - 1/\tau_{open}$; k_{ET} = 2.64 $\times 10^9$ s^{-1} and 2.30$\times 10^9$ s^{-1} for **ICP1** and **ICP2**), assuming that the photophysical processes inherent to **L1** and **L2** were unaffected by the photochromism of **L3**. It is noted that the rate constants for energy transfer are much larger than those for radiative and non-radiative decay rates (SI, Figure S10).The faster energy transfer in **ICP2** can be explained on the basis of the higher FRET efficiency (η_{ICP2} = 0.76) than that of **ICP1** (η_{ICP1} = 0.69) calculated by $\eta = 1 - \tau_{off} / \tau_{on}$ (τ_{off} and τ_{on} are the average fluorescence lifetimes of the closed and open form of ICPs). The Förster radii calculated for the former and the latter pairs are R_0 = 14.82 Å and 12.58 Å for **ICP1** and **ICP2**, respectively. Since the distances between **L3** and **L1** (or **L2**) in ICPs (R = ~3.6 Å, calculated using B3LYP/6-31G**) would be short enough compared to the Förster radii (R/R_0 = ~0.26), the occurrence of highly efficient interligand energy transfer is anticipated. It should be noted that we could not decide the specific value of the orientation factor explicitly even we could obtain the suggested structure of ICPs through XPS and GIXD. Therefore, we assumed our ICPs has random orientation. The Förster radii calculated for the former and the latter pairs are R_0 = 14.82 Å and 12.58 Å for **ICP1** and **ICP2**, respectively. Since the distances between **L3** and **L1** (or **L2**) in ICPs (R = ~3.6 Å, calculated using B3LYP/6-31G**) would be short enough compared to the Förster radii (R/R_0 = ~0.26), the occurrence of highly efficient interligand energy transfer is anticipated.

In summary, we have designed and synthesized novel reconfigurable ICPs which are capable of optical switching of solid-state fluorescence. The ICPs contained two types of bridging ligands with different function, i.e., photochromic and AIEE-fluorescent ligands. Well-ordered crystalline micropatterns were fabricated by taking advantage of the MIMIC method and the reversible nature of the coordination bonds. The multidimensional superstructures in the ICP micropatterns were analysed using various spectroscopic techniques, including 2D GIXD. The ICP micropatterns exhibited high contrast, reversible modulation of photoluminescence emission, enabling true solid-state all-optical memory. Steady-state and transient PL studies indicated that the photoluminescence modulation was due to the interligand energy transfer.

Acknowledgements

This work was supported by the National Research Foundation of Korea (NRF) grant funded by the Korea government (MSIP; No. 2009-0081571[RIAM0417-20150013])

Keywords: photochromism • coordination polymers • nanostructures • fluorescence • micromolding

[1] a) S. Kitagawa, R. Kitaura and S. Noro, *Angewandte Chemie-International Edition* **2004**, *43*, 2334-2375; b) J. M. Lehn, *Science* **2002**, *295*, 2400-2403; c) B. Moulton and M. J. Zaworotko, *Chemical Reviews* **2001**, *101*, 1629-1658; d) Q. L. Zhu and Q. Xu, *Chemical Society Reviews* **2014**, *43*, 5468-5512; e) O. M. Yaghi, H. L. Li and T. L. Groy, *Inorganic Chemistry* **1997**, *36*, 4292-4293; f) M. E. Kosal, J. H. Chou, S. R. Wilson and K. S. Suslick, *Nature Materials* **2002**, *1*, 118-121.

[2] a) L. J. Murray, M. Dinca and J. R. Long, *Chemical Society Reviews* **2009**, *38*, 1294-1314; b) J. A. Mason, M. Veenstra and J. R. Long, *Chemical Science* **2014**, *5*, 32-51; c) K. Nakagawa, D. Tanaka, S. Horike, S. Shimomura, M. Higuchi and S. Kitagawa, *Chemical Communications* **2010**, *46*, 4258-4260; d) T. Fukushima, S. Horike, Y. Inubushi, K. Nakagawa, Y. Kubota, M. Takata and S. Kitagawa, *Angewandte Chemie-International Edition* **2010**, *49*, 4820-4824; e) F. Zhang, X. Q. Zou, X. Gao, S. J. Fan, F. X. Sun, H. Ren and G. S. Zhu, *Advanced Functional Materials* **2012**, *22*, 3583-3590; f) H. Sato, W. Kosaka, R. Matsuda, A. Hori, Y. Hijikata, R. V. Belosludov, S. Sakaki, M. Takata and S. Kitagawa, *Science* **2014**, *343*, 167-170.

[3] D. E. Williams, J. A. Rietman, J. M. Maier, R. Tan, A. B. Greytak, M. D. Smith, J. A. Krause and N. B. Shustova, *Journal of the American Chemical Society* **2014**, *136*, 11886-11889.

[4] a) R. K. Das, A. Aijaz, M. K. Sharma, P. Lama and P. K. Bharadwaj, *Chemistry-a European Journal* **2012**, *18*, 6866-6872; b) F. X. Bu, M. Hu, L. Xu, Q. Meng, G. Y. Mao, D. M. Jiang and J. S. Jiang, *Chemical Communications* **2014**, *50*, 8543-8546.

[5] a) L. Xing, H. Q. Zheng, Y. Y. Cao and S. A. Che, *Advanced Materials* **2012**, *24*, 6433-6437; b) I. Imaz, M. Rubio-Martinez, L. Garcia-Fernandez, F. Garcia, D. Ruiz-Molina, J. Hernando, V. Puntes and D. Maspoch, *Chemical Communications* **2010**, *46*, 4737-4739; c) I. Imaz, J. Hernando, D. Ruiz-Molina and D. Maspoch, *Angewandte Chemie-International Edition* **2009**, *48*, 2325-2329.

[6] a) N. Yanai, K. Kitayama, Y. Hijikata, H. Sato, R. Matsuda, Y. Kubota, M. Takata, M. Mizuno, T. Uemura and S. Kitagawa, *Nature Materials* **2011**, *10*, 787-793; b) Y. Takashima, V. M. Martinez, S. Furukawa, M. Kondo, S. Shimomura, H. Uehara, M. Nakahama, K. Sugimoto and S. Kitagawa, *Nature Communications* **2011**, *2, 168*; c) Y. Li, K. Liu, W. J. Li, A. Guo, F. Y. Zhao, H. Liu and W. J. Ruan, *Journal of Physical Chemistry C* **2015**, *119*, 28544-28550; d) H. L. Tan, B. X. Liu and Y. Chen, *Acs Nano* **2012**, *6*, 10505-10511; e) M. M. Chen, X. Zhou, H. X. Li, X. X. Yang and J. P. Lang, *Crystal Growth & Design* **2015**, *15*, 2753-2760.

[7] a) J. C. Dai, X. T. Wu, Z. Y. Fu, C. P. Cui, S. M. Hu, W. X. Du, L. M. Wu, H. H. Zhang and R. O. Sun, *Inorganic Chemistry* **2002**, *41*, 1391-1396; b) J. Zhang, Y. R. Xie, Q. Ye, R. G. Xiong, Z. L. Xue and X. Z. You, *European Journal of Inorganic Chemistry* **2003**, 2572-2577; c) K. C. Stylianou, R. Heck, S. Y. Chong, J. Bacsa, J. T. A. Jones, Y. Z. Khimyak, D. Bradshaw and M. J. Rosseinsky, *Journal of the American Chemical Society* **2010**, *132*, 4119-4130; d) N. B. Shustova, B. D. McCarthy and M. Dinca, *Journal of the American Chemical Society* **2011**, *133*, 20126-20129; e) Y. J. Cui, W. F. Zou, R. J. Song, J. C. Yu, W. Q. Zhang, Y. Yang and G. D. Qian, *Chemical Communications* **2014**, *50*, 719-721; f) J. Mei, N. L. C. Leung, R. T. K. Kwok, J. W. Y. Lam and B. Z. Tang, *Chemical Reviews* **2015**, *115*, 11718-11940; g) A. Fermi, G. Bergamini, M. Roy, M. Gingras and P. Ceroni, *Journal of the American Chemical Society* **2014**, *136*, 6395-6400; h) V. Sathish, A. Ramdass, P. Thanasekaran, K. L. Lu and S. Rajagopal, *Journal of Photochemistry and Photobiology C-Photochemistry Reviews* **2015**, *23*, 25-44.

[8] Y. You, H. Yang, J. W. Chung, J. H. Kim, Y. Jung and S. Y. Park, *Angewandte Chemie-International Edition* **2010**, *49*, 3757-3761.

[9] a) M. Irie, *Chemical Reviews* **2000**, *100*, 1685-1716; b) S. J. Lim, B. K. An, S. D. Jung, M. A. Chung and S. Y. Park, *Angewandte Chemie-International Edition* **2004**, *43*, 6346-6350; c) S. J. Lim, B. K. An and S. Y. Park, *Macromolecules* **2005**, *38*, 6236-6239; d) J. W. Chung, S. J. Yoon, S. J. Lim, B. K. An and S. Y. Park, *Angewandte Chemie-International Edition* **2009**, *48*, 7030-7034.

[10] S. Kim, S. J. Yoon and S. Y. Park, *Journal of the American Chemical Society* **2012**, *134*, 12091-12097.

[11] a) S. L. Gilat, S. H. Kawai and J. M. Lehn, *Chemistry-a European Journal* **1995**, *1*, 275-284; b) B. K. An, S. K. Kwon, S. D. Jung and S. Y. Park, *Journal of the American Chemical Society* **2002**, *124*, 14410-14415.

[12] a) J. Ruokolainen, J. Tanner, G. Tenbrinke, O. Ikkala, M. Torkkeli and R. Serimaa, *Macromolecules* **1995**, *28*, 7779-7784; b) L. A. Belfiore, A. T. N. Pires, Y. H. Wang, H. Graham and E. Ueda, *Macromolecules* **1992**, *25*, 1411-1419.

[13] M. Morimoto and M. Irie, *Chemical Communications* **2005**, 3895-3905.